AFRL-RZ-WP-TR-2011-2082

DISPERSION STRENGTHENING OF FE-CO ALLOYS FOR HIGH TEMPERATURE APPLICATIONS

Robert Cammarata

Johns Hopkins University

March 2011
Final Report

Approved for public release; distribution unlimited.

See additional restrictions described on inside pages

AIR FORCE RESEARCH LABORATORY
PROPULSION DIRECTORATE
WRIGHT-PATTERSON AIR FORCE BASE, OH 45433-7251
AIR FORCE MATERIEL COMMAND
UNITED STATES AIR FORCE

NOTICE AND SIGNATURE PAGE

AFRL-RZ-WP-TR-2011-2082 HAS BEEN REVIEWED AND IS APPROVED FOR PUBLICATION IN ACCORDANCE WITH ASSIGNED DISTRIBUTION STATEMENT.

*//Signature//
Earl M Gregory
Project Engineer
Mechanical Energy Conversion Branch

//Signature//
Jack U Vondrell
Chief
Mechanical Energy Conversion Branch

REPORT DOCUMENTATION PAGE

Form Approved
OMB No. 0704-0188

1. REPORT DATE *(DD-MM-YYYY)* **Mar 2011**	**2. REPORT TYPE** **Final Report**	**3. DATES COVERED** *(From - To)* 26 Apr 07 - 26 Dec 10

4. TITLE AND SUBTITLE
Dispersion Strengthening of Fe-Co Alloys for High Temperature Applications

5a. CONTRACT NUMBER **FA8650-07-2-2738**
5b. GRANT NUMBER
5c. PROGRAM ELEMENT NUMBER **62203F**

6. AUTHOR(S)
Robert C. Cammarata and Chia-Ling Chien

5d. PROJECT NUMBER **3145**
5e. TASK NUMBER **G1**
5f. WORK UNIT NUMBER **3145G105**

7. PERFORMING ORGANIZATION NAME(S) AND ADDRESS(ES)
Johns Hopkins University
3400 N Charles Street Rm 249
Baltimore, MD 21218-2680

8. PERFORMING ORGANIZATION REPORT

9. SPONSORING / MONITORING AGENCY NAME(S) AND ADDRESS(ES)
Air Force Research Laboratory
Propulsion Directorate
Wright-Patterson AFB, OH 45433-7251
Air Force Materiel Command
United States Air Force

10. SPONSOR/MONITOR'S ACRONYM(S) **AFRL/RZPG**

11. SPONSOR/MONITOR'S REPORT NUMBER(S) **AFRL-RZ-WP-TR-2011-2082**

12. DISTRIBUTION / AVAILABILITY STATEMENT
Approved for public release; distribution is unlimited.
Public Release 88ABW 2011-3402, 14 Jun 2011

13. SUPPLEMENTARY NOTES
Report contains color

14. ABSTRACT
The overall objective of this effort was to increase tield strength and creep resistance of Fe-Co based alloys for applications at elevated temperatures. The project focused on two main areas: (i) inducing grain growth by annealing of as-rolled Hiperco 50 HS alloys from Carpenter Technology Corporation in order to improve creep resistance; (ii) optimizing a novel electrochemical deposition process to produce oxide dispersion strengthened materials. Results have shown that large grain size FeCo alloys can display both the yield strength and creep behavior desired for high temperature rotating machine applications without significant degradation of the magnetic properties.

15. SUBJECT TERMS:
Large grain FeCo, High Temperature, Oxide dispersion strengthening

16. SECURITY CLASSIFICATION OF: a. REPORT	b. ABSTRACT	c. THIS PAGE	17. LIMITATION OF ABSTRACT	18. NUMBER OF PAGES	19a. NAME OF RESPONSIBLE PERSON / 19b. TELEPHONE NUMBER *(include area code)*
Unclassified	Unclassified	Unclassified	SAR	22	Earl Gregory / 937-255-6205

Standard Form 298 (Rev. 8-98)
Prescribed by ANSI Std. 239.18

Table of Contents

List of Figures

List of Tables

1.0 Executive Summary

This report presents the principal results obtained from our research on improving the yield strength and creep resistance of FeCo-based alloys for elevated temperature magnetic bearing applications. This work has proceeded in two areas: (i) inducing grain growth by annealing of as-rolled Hiperco 50HS alloys obtained from Carpenter Technology Corp. in order to improve the creep resistance; (ii) optimizing a novel electrochemical deposition process to produce oxide dispersion strengthened materials. We have shown that large grain size FeCo alloys can display both the yield strength and creep behavior desired for high temperature magnetic applications without significant degradation of the magnetic properties. Annealing Hiperco 50HS FeCo at 1200°C for one hour resulted in an average grain size of 161μm. In addition, a subgrain microstructure of average subgrain size 10μm was produced along with precipitation of second phase particles at the subgrain boundaries. Preliminary analysis indicated that the precipitates were niobium carbide. This unique microstructure resulted in very much enhanced creep rates at temperatures up to 600°C. Much of the yield strength lost owing to the increase in grain size was regained in the larger grain size materials, apparently owing to the subgrain structure and reinforcing second phase precipitates. Thus, this simple processing of commercially available alloys has produced materials displaying properties very near that desired for high temperature military applications. Further work optimizing the annealing schedule and resulting microstructure should produce even greater improvements. The synthesis of oxide dispersion strengthened, metal matrix composites by a novel electrochemical deposition process using a rotating disk electrode that displays enhanced mechanical properties without significant degradation of the magnetic properties has been demonstrated for a nickel-based system. Difficulties were encountered in attempting to extend this method to FeCo. Although we believe this method still holds promise for the FeCo system, more development work is needed.

2.0 Introduction

Owing to its superior magnetic properties, FeCo-based alloys have attracted a great deal of interest for their application as soft magnets components such as rotors in magnetic bearings in propulsion engines. For many of these applications, the alloys are subjected to an extreme environment of high stress and high temperature. As a result, these materials must possess both high mechanical strength and low creep rate at elevated temperatures; behaviors that are lacking in currently employed materials. The challenge is to develop synthesis and/or processing methods that significantly improve the mechanical properties of these FeCo-based systems while not adversely affecting the superior soft magnetic properties.

Although a great deal of work has been conducted during the several past decades on the yield strength of FeCo-based alloys, there has been much less attention paid to the creep properties. There is general agreement that the primary creep mechanism is power law (dislocation) creep, which is relatively less well understood compared to diffusional (Nabarro- Herring and Coble) creep. Empirically it has been observed in several metallic systems that the creep resistance is sensitively dependent on certain microstructural features.

Strengthening by the introduction of second phase oxide particles has been shown to be one method of enhancing both the yield strength and creep resistance. This can be understood as resulting from the oxide particles acting as obstacles to dislocation glide. It has also been shown that for many metallic systems increasing the grain size by, for example, inducing grain growth through thermal annealing, can exponentially enhance the creep resistance. The reason for this behavior is not well understood. Concomitant with this behavior is reduced yield strength owing to the reduction in the grain boundary (Hall-Petch) hardening. Thus, it is expected that if increased grain size is employed to improve the creep properties it will be necessary to address the associated reduction in the yield strength by some other hardening mechanism.

3.0 Methods, Assumptions and Procedures

3.1 Mechanical Strengthening Strategies We have pursued two strategies for producing FeCo-based alloys with enhanced mechanical properties. The first involved subjecting commercially available Hiperco 50HS sheets to annealing treatments that induced grain growth. Originally the aim was to characterize the relationships between grain size and creep resistance at elevated temperatures, as well as room temperature yield strength. As was mentioned above, it was anticipated that while the creep resistance would increase, the yield strength would decrease, owing to grain growth. However, our results showed that both creep resistance and yield strength increased after certain annealing treatments, ultimately reaching values very close to that needed for military applications. This exciting and unexpected behavior is believed to be a result of unique microstructural features as discussed below.

3.2 The second strengthening strategy was to produce oxide-strengthened FeCo materials by a novel electrochemical deposition method employing a rotating disk electrode. Although it was not expected that this approach would be practical as a synthesis method for actual materials to be used in the field, it was hoped that it could be used to produce samples for proof of concept testing. Results obtained from the annealed Hiperco materials will first be presented; this will be followed by a discussion of the electrodeposition process.

4.0 Results and Discussion

4.1 Annealed Hiperco Alloys Annealing treatments on Hiperco 50HS FeCo alloys were conducted to induce grain growth. The 50HS system was selected as it has displayed excellent magnetic properties as well as good room temperature yield strength. The furnace anneals were conducted under reducing atmosphere conditions.

4.2 Microstructure. Figure 1 shows a bright field transmission electron micrographs (TEM) of an Hiperco 50HS FeCo alloys subjected to an anneal at 700°C for four hours. It is seen that this anneal produced equiaxed grains of about 0.3 μm average grain size. Figure 2 shows a bright field TEM of a sample annealed at 700°C for 4hr displaying an average grain size of about 0.7μm. Figures 3-6 are optical micrographs for alloys annealed at 843°C for 2hr, 1000°C for 1hr, 1100°C for 1hr, and 1200°C for 1 hr, respectively. The average grain size ranged from about 10μm in Figure 3 to 161μm in Figure 6. Figure 7-9 are bright field TEM for alloys annealed at 1200°C for 1hr, producing an average grain size of 161μm. It is seen that a subgrain microstructure developed with what appeared to be precipitate particles formed at the subgrain boundaries. Preliminary energy-dispersive X-ray spectroscopy (EDS) analysis indicated that these particles contained a large concentration of Nb; we speculate that the particles are niobium carbide. As discussed below, the presence of the subgrain structure and reinforcing precipitate particles may be responsible for the enhanced yield strength and may also contribute to the improved creep resistance.

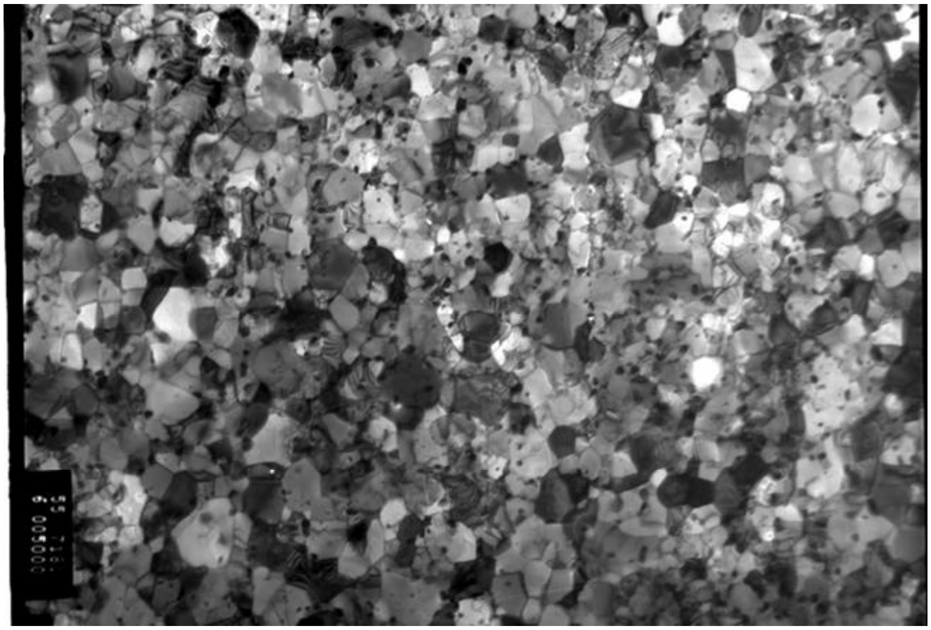

Figure 1. Bright field TEM of an Hiperco 50HS alloy subjected to an anneal of 650°C for 4hr. Average grain size of about 0.3μm.

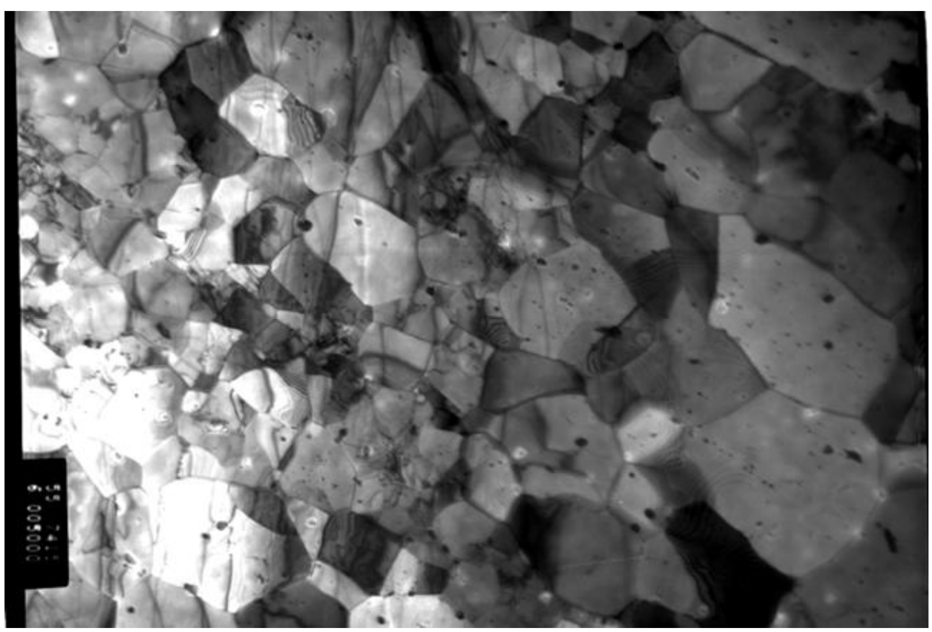

Figure 2. Bright field TEM of an Hiperco 50HS alloy subjected to an anneal of 700°C for 4hr. Average grain size of about 0.7μm.

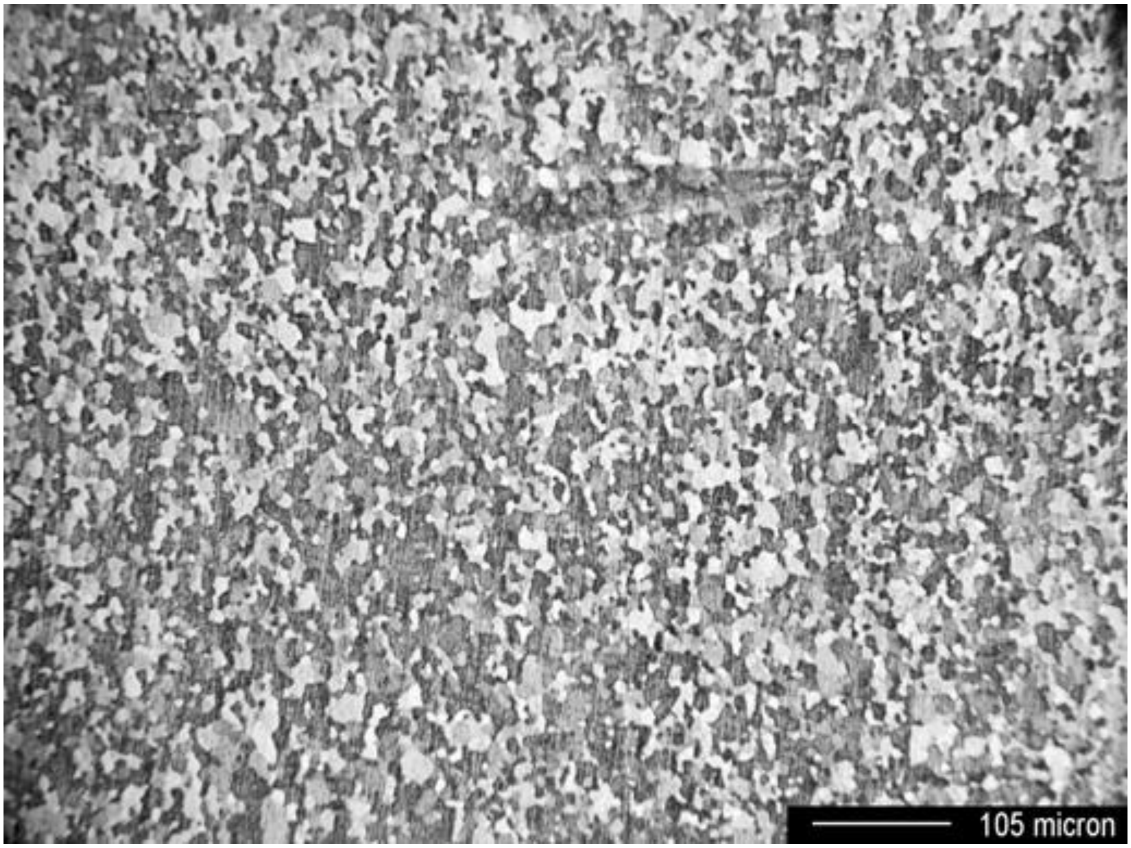

Figure 3. Optical micrograph of an Hiperco 50HS alloy subjected to an anneal of 843°C for 2hr. Average grain size of about 10µm.

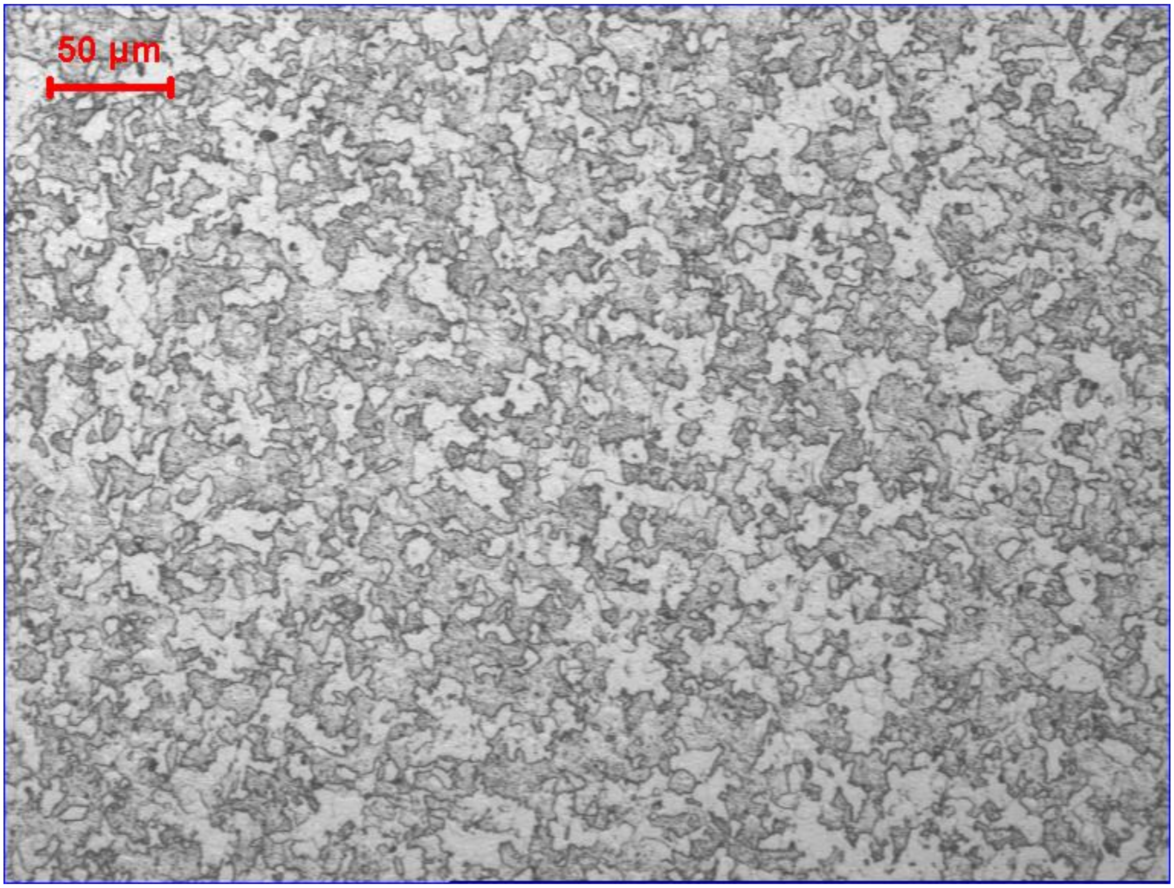

Figure 4. Optical micrograph of an Hiperco 50HS alloy subjected to an anneal of 1000°C for 1hr. Average grain size of about 16µm.

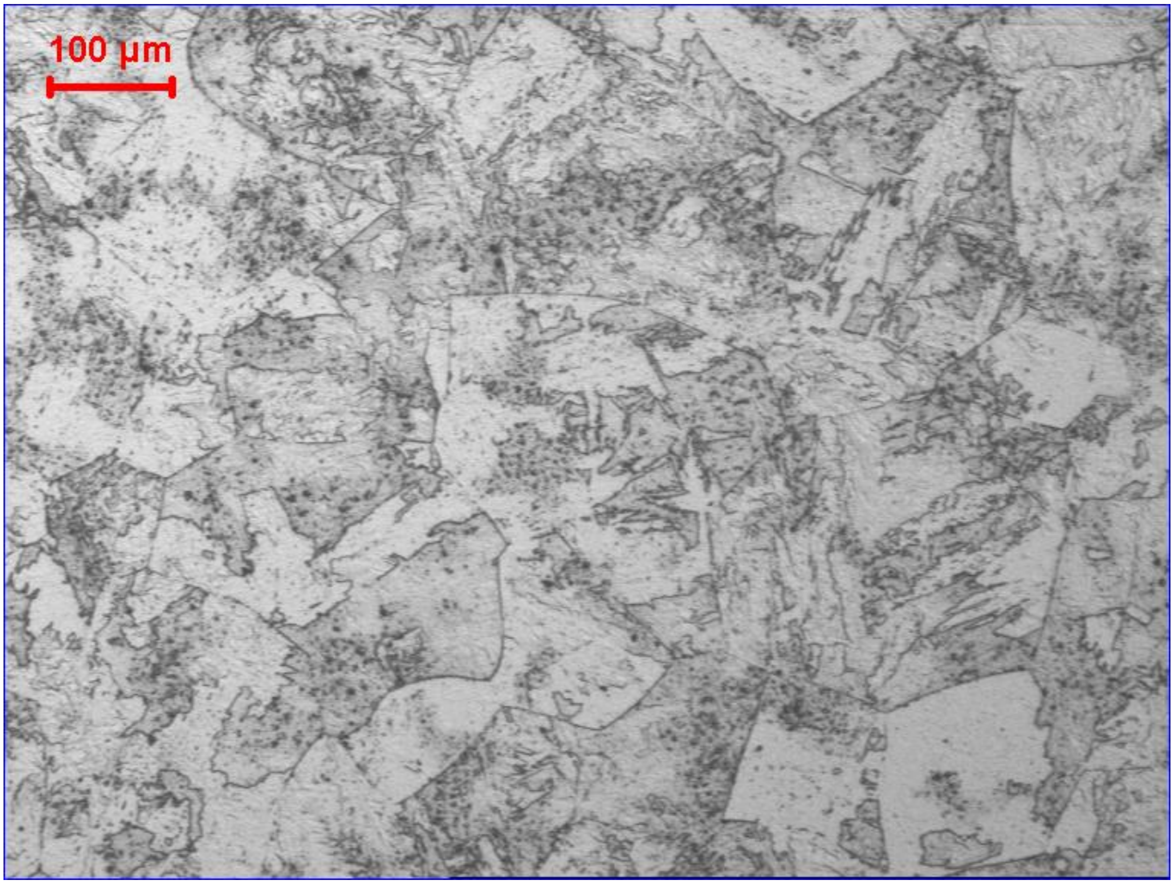

Figure 5. Optical micrograph of an Hiperco 50HS alloy subjected to an anneal of 1100°C for 1hr. Average grain size of about 70µm.

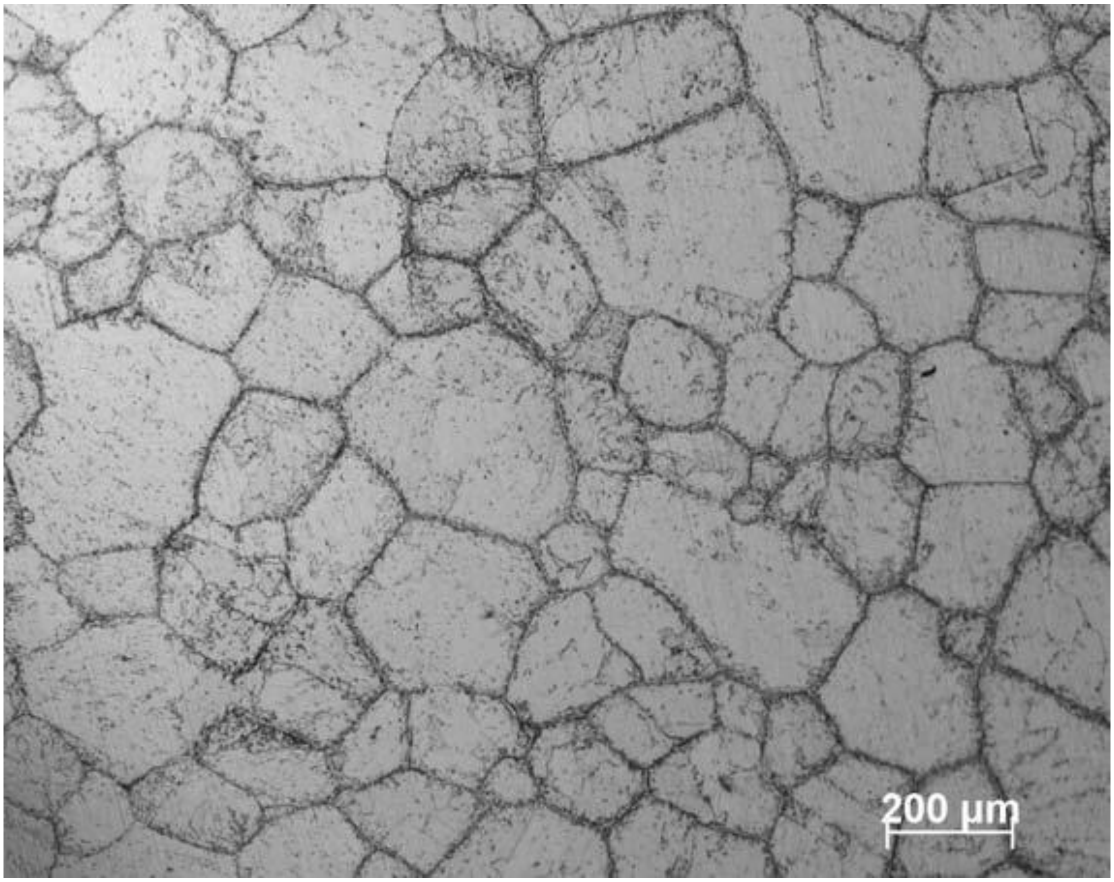

Figure 6. Optical micrograph of Hiperco 50HS alloy subjected to an anneal of 1200°C for 1hr. Average grain size of about 161µm.

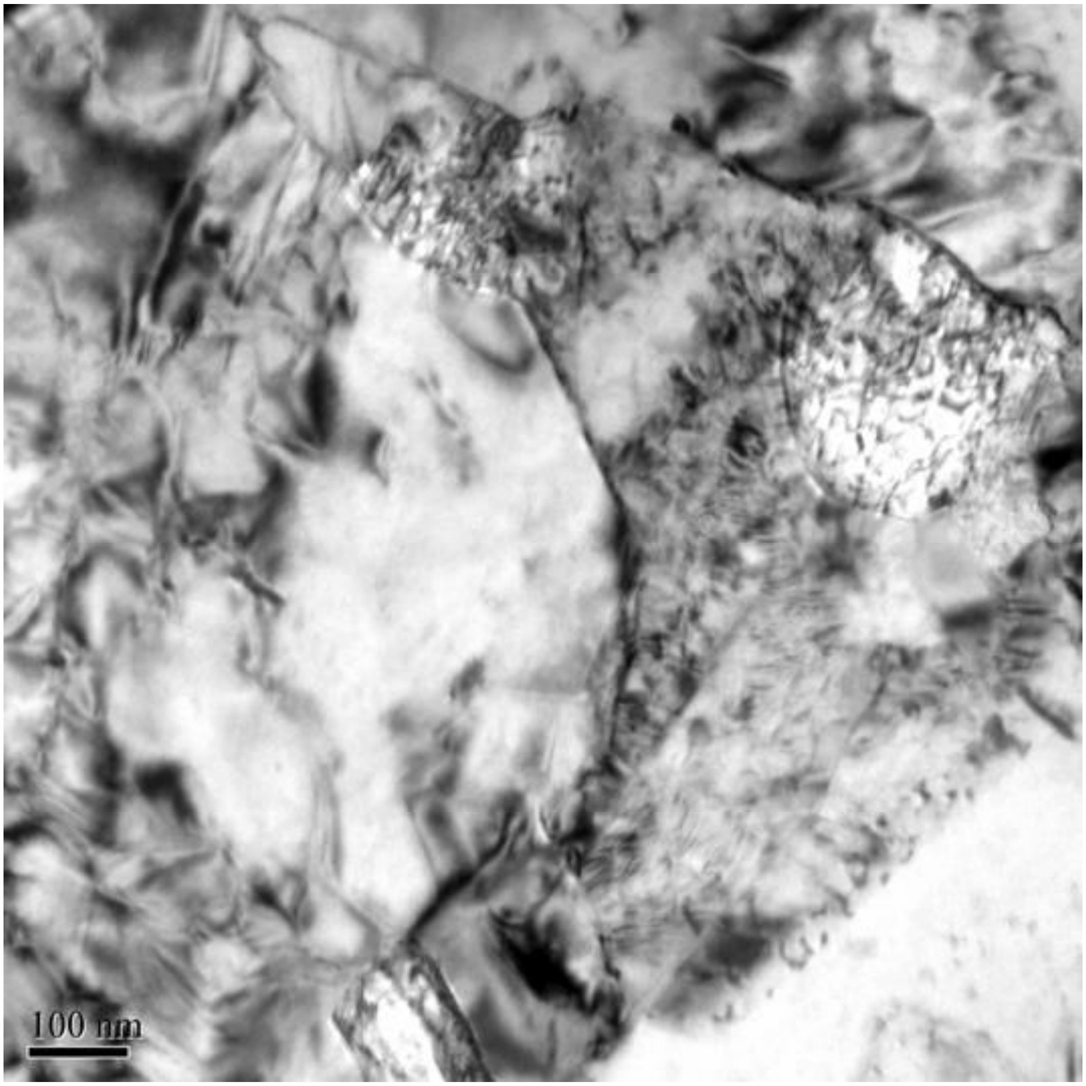

Figure 7. Bright field TEM of Hiperco 50HS alloy subjected to an anneal of 1200°C for 1hr. Average grain size of about 161μm. A subgrain structure is displayed.

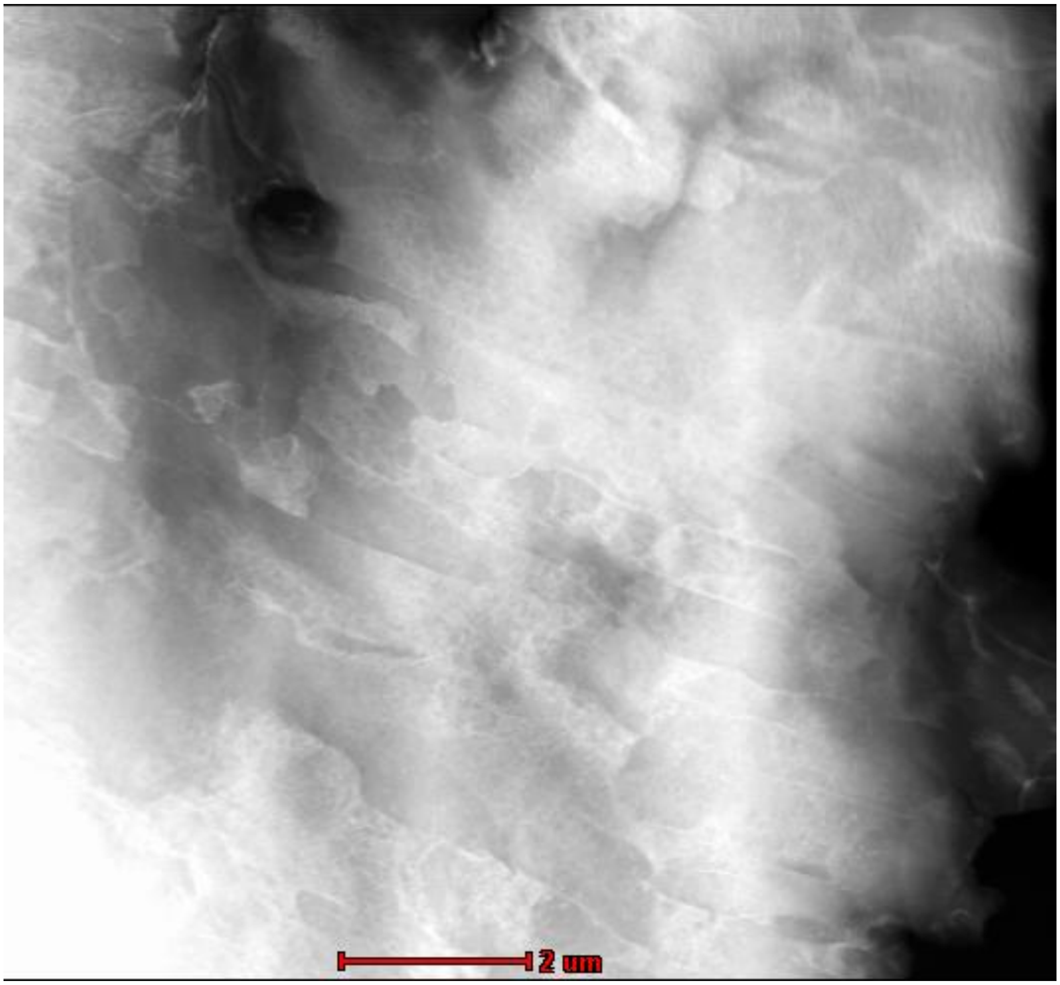

Figure 8. Higher magnification dark field TEM of an Hiperco 50HS alloy subjected to an anneal of 1200°C for 1hr displaying subgrain of size about 1μm.

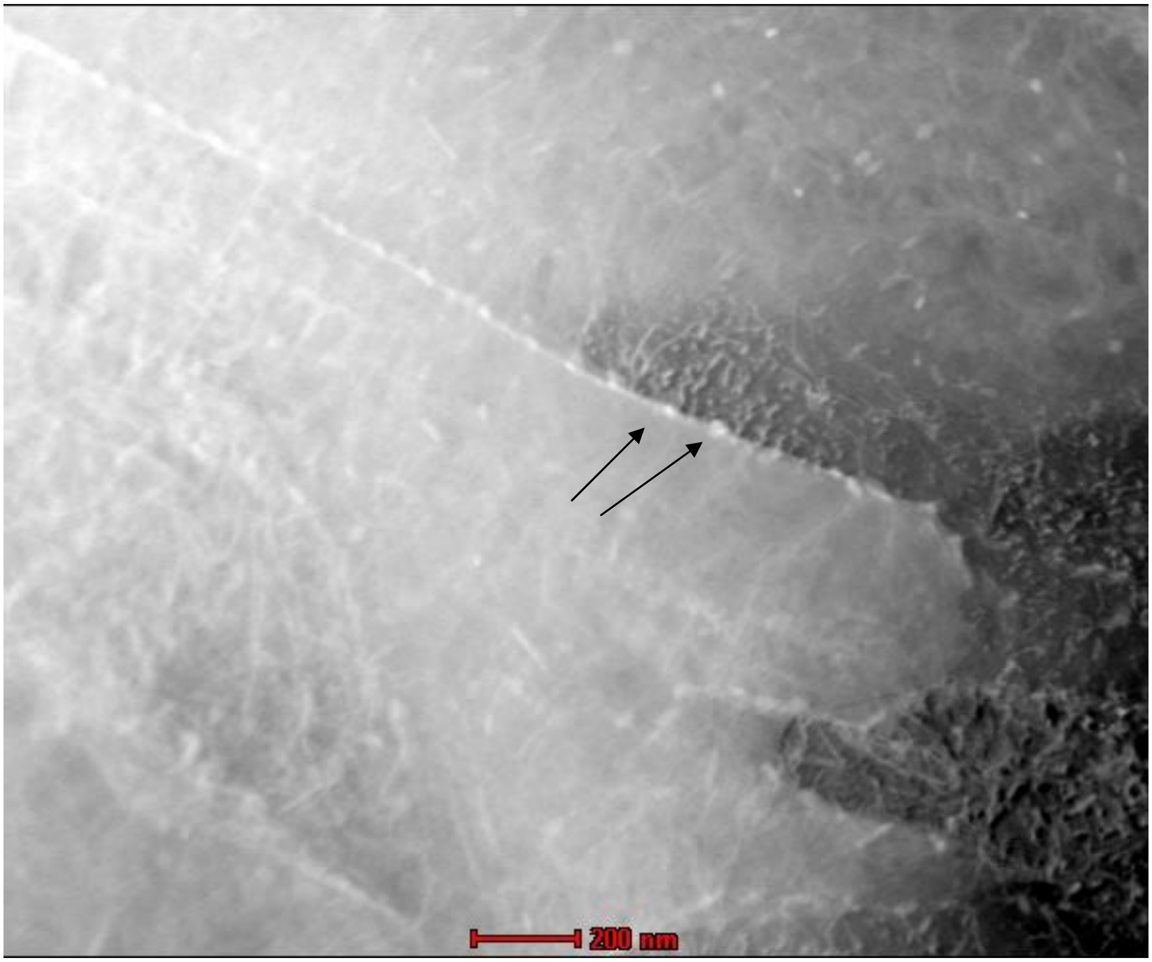

Figure 9. Bright field TEM of Hiperco 50HS alloy subjected to an anneal of 1200°C for 1hr. Arrows point to apparent precipitates at the subgrain boundaries.

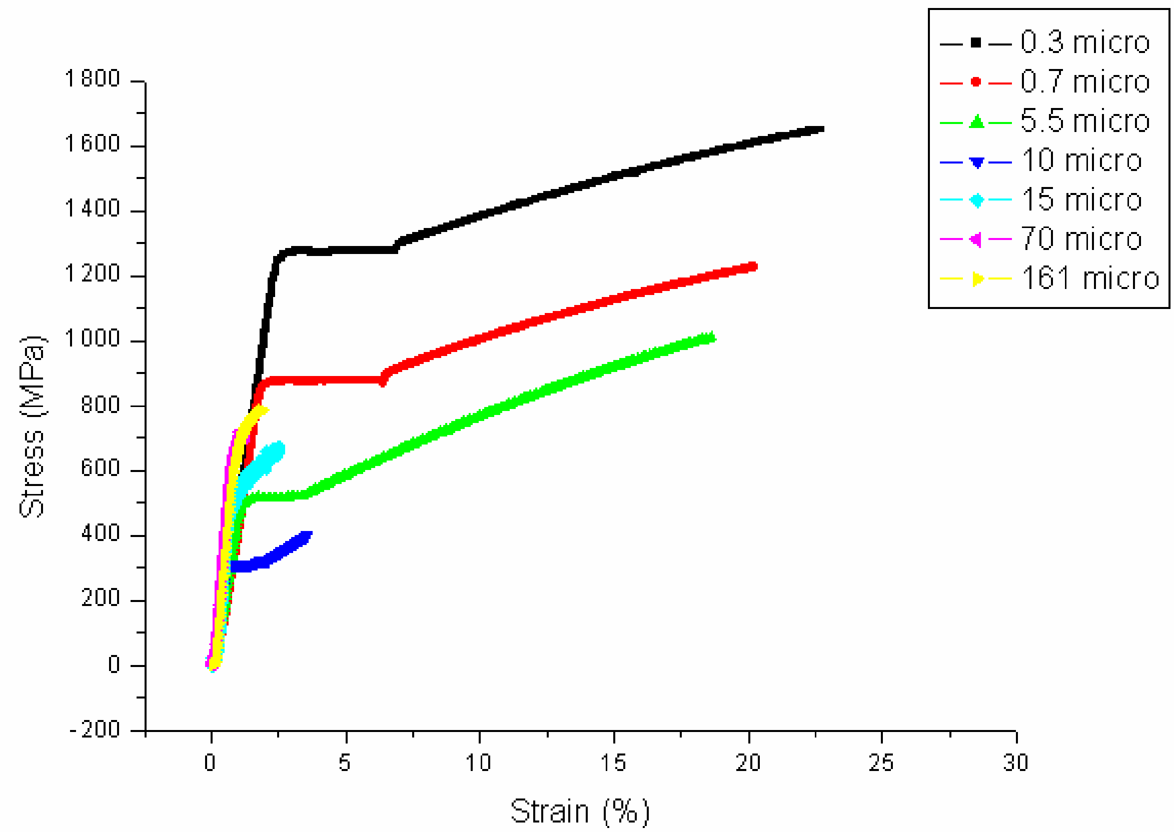

Figure 10. Room temperature tensile stress-strain curves for annealed 50HS alloys with different grain sizes.

Heat treatment	Grain size (µm)	Yield strength (MPa)	Ultimate strength (MPa)	Elongation (%)
650°C (4hr)	0.3	1273	1649	18
700°C (4hr)	0.7	876	1226	17.5
750°C (4hr)	5.5	516	1010	16.6
843°C (2hr)	10	306	400	2.9
1000°C (1hr)	15	510	661	1.7
1100°C (1hr)	70	687	717	0.6
1200°C (1hr)	161	701	824	1.4

Table 1. Yield and ultimate tensile strengths for annealed 50HS alloys of different grain sizes.

4.3 Tensile Stress-Strain Tests Figure 10 shows a comparison of room temperature tensile stress-strain curves obtained from annealed 50HS alloys with different grain sizes. Table 1 gives the yield and ultimate tensile strengths for these alloys. Unlike previous studies in which annealed alloys displayed Hall- Petch-type behavior (i.e., reduced yield strength with increased grain size), in this study there is no simple correlation of strength with grain size. While initially increasing the grain size does result in softening, further grain size increases are accompanied by increased strengthening. This suggests that hardening effects due to the subgrain structure and precipitates, observed during the high temperature anneals, return some of the strengthening lost due to the grain size increase.

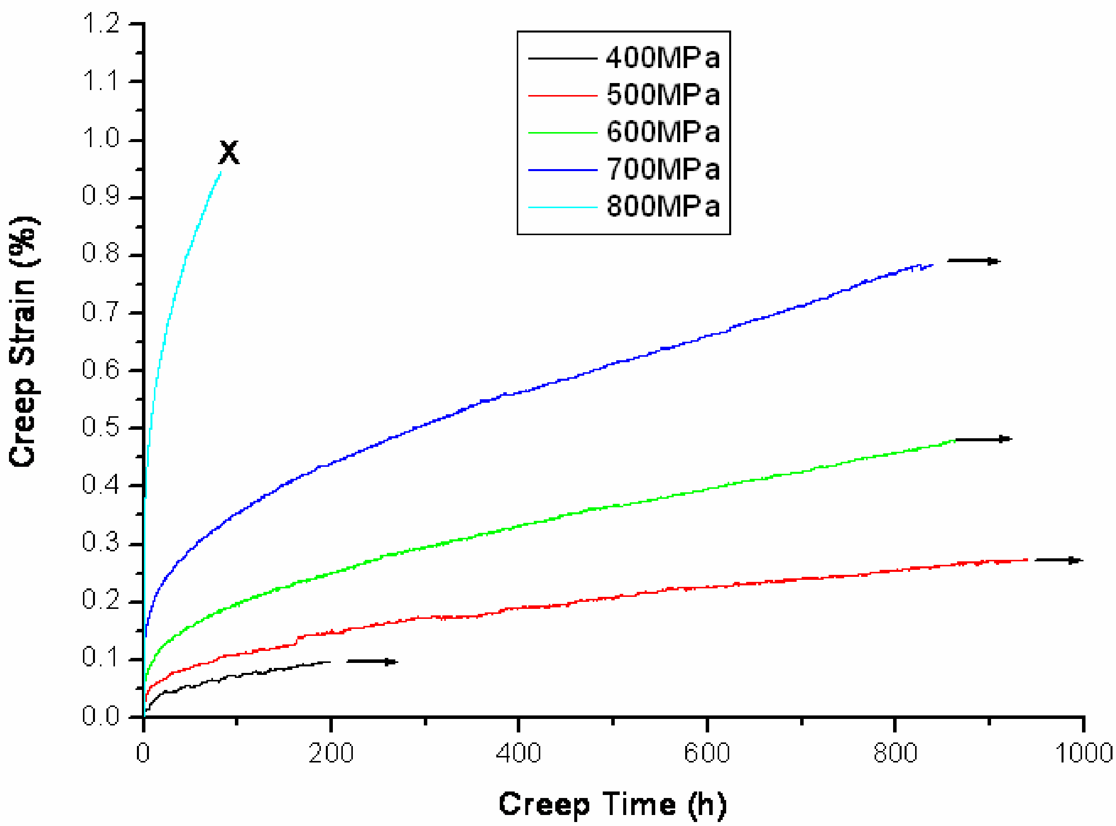

Figure 11. Creep strain for different applied stresses at 500°C as a function of time for Hiperco 50HS with average grain size of 161µm.

Stress (MPa)	400C(1/s) *10^{-11}	500C(1/s) *10^{-10}	550C(1/s) *10^{-9}	600C(1/s) *10^{-8}
300				3.3
350				12
400			8.1	36
500	8.6	4.2	18	83
600	9.2	8.9	31	
700		15	72	
800		110		

Table 2. Creep rates for different applied stresses and temperatures for Hiperco 50HS with average grain size of 161μm.

4.4 Creep testing went as expected, the largest grain size samples (161μm) displayed the greatest creep resistance for a given temperature. Figure 11 shows the creep strain for different applied stresses at 500°C as a function of time for this alloy. Table 2 shows the creep rates for different applied stresses and temperatures. It is seen that this largest grain size material displayed creep rates very close to the high creep resistance properties required for military applications. With further refinements in the annealing process to produce the optimal microstructure composed of a large overall grain size, a smaller subgrain structure, and reinforcing second phase precipitates, even greater enhancements in both yield and creep strength should be achievable.

4.5 Oxide-Dispersion Strengthened Electrodeposited Alloys. Using a novel rotating disk electrode electrochemical deposition system, we have been able to produce nickel-matric materials with a second phase oxide dispersion. The nickel electrolyte in which the electrodeposition took place contained a suspension of oxide particles that under the influence of the rotating disk electrode became embedded in the growing metal. The volume fraction of the oxide could be sensitively controlled by adjusting the oxide concentration in the electrolyte, the deposition current density, and the electrode rotation rate. The resulting metal-oxide composite displayed significant hardness enhancements compared to the single phase nickel with little degradation of the magnetic properties. We were able to perfect the electrodeposition of relatively large area and thickness FeCo alloy films in the absence of an oxide dispersion; however, difficulties were encountered attempting to deposit FeCo with the oxide dispersion. We are currently working with collaborators at IBM-Yorktown Heights to overcome these difficulties.

5.0 Conclusions

As previously discussed, we have obtained exciting results indicating that it is possible, using the proper annealing treatment on commercially available Hiperco alloys, to obtain the required creep resistance and yield strength, as well as magnetic properties, for high temperature military applications. Thus, it may not be necessary to develop materials with an oxide dispersion. TEM microstructural studies indicate that the annealed alloy has a subgrain microstructure and that small precipitates have formed, particularly at the subgrain boundaries. It is believed these features result in the enhanced mechanical properties.

6.0 Recommendations

Further materials work is needed in order to determine the strengthening mechanisms in more detail as well as the stability of the microstructure. It is also suggested that a small scale rotating machine prototype be constructed from this new annealed material, and be tested at various elevated temperature conditions to see how it performs in a real world application.

7.0 References

C.H. Shang, R.C. Cammarata, T.P. Weihs, C.L. Chien, "Microstructure and Hall-Petch Behavior of FeCo-based Hiperco Alloys," J. Mater. Res. **15**, 835 (2000).

C.H. Shang, T. P. Weihs, R. C. Cammarata, Y. Ji and C. L. Chien, "Anisotropy in Magnetic and Mechanical Properties in Textured Hiperco FeCoV Alloys," J. Appl. Phys. **87**, 6508 (2000).

A. Duckham, D. Zhang, R.C. Cammarata, C.L. Chien and T.P. Weihs, Temperature Dependent Mechanical Properties of Ultrafine-Grained FeCo-2V, Acta Materialia, **51**, 4083 (2003).

X.M. Cheng, X.K. Zhang, D.Z. Zhang, S.H. Lee, A. Duckham, T.P. Weihs, R.C. Cammarata, J.Q. Xiao, and C.L. Chien, “Magnetic Core Loss of Ultrahigh Strength Nanocrystalline FeCo Alloys,” J. Appl. Phys. **93**, 7121 (2003).

I. Shao, P.M. Vereecken, P.C. Searson, C.L. Chien, and R.C. Cammarata, "Electrochemical Deposition of Nanocomposite Soft Magnetic Materials," Proceedings 6th International Symposium on Magnetic Materials, Processes and Devices, Editors S. Krongelb, L.T. Romankiw, J.-W. Chang, W. Schwarzacher, and C.H. Ahn, Proceedings Volume PV 2000-29, The Electrochemical Society, Pennington, New Jersey.(2001) p. 420.

I. Shao, P.M. Vereecken, R. C. Cammarata, P.C. Searson, and C.L. Chien, "ElectrochemicalDeposition of FeCo Alloys and FeCo/TiO_2 Nanocomposites," Mater. Res. Symo. Proc. **674**, U53 (2001).

I. Shao, P. M. Vereecken, C. L. Chien, R. C. Cammarata, and P. C. Searson, "Magnetic and Mechanical Properties of Ni/Al2O3 Nanocomposite Films," J. Mater. Res., **17**, 1412 (2002).

C.H. Shang, R.C. Cammarata, D. Van Heerden, C.L.Chien, and T.P. Weihs, ”Bulk Processing of High Performance Nanocrystalline FeCo Intermetallics,” J. Mater. Res. 18, 2017-2020, (2003).

T.P. Weihs, R.C. Cammarata, C.L. Chien, and C.H. Shang, “High performance nanostructured materials and methods of making the same,” U.S. Patent 6,596,101, awarded July 23, 2003.

List of Symbols, Abbreviations, and Acronyms

EDS	Energy-dispersive X-ray spectroscopy
TEM	Transmission electron micrographs